




Cite this: *Org. Biomol. Chem.*, 2018, **16**, 5036

A red-emitting fluorescent probe for the detection of Hg^{2+} in aqueous medium, living cells and organisms with a large Stokes shift†

Lei Yang,[‡] Yuanan Su,[‡] Yani Geng, Haiqing Xiong, Jinliang Han, Qian Fang and Xiangzhi Song *

Received 9th April 2018,
Accepted 14th May 2018

DOI: 10.1039/c8ob00831k

rsc.li/obc

A red-emitting fluorescent probe has been developed for the selective and sensitive detection of Hg^{2+} . With the addition of Hg^{2+} , the solution of probe **1** displayed a remarkable fluorescence enhancement (102 fold) with $\lambda_{\text{max}}^{\text{em}} = 625 \text{ nm}$ and a large Stokes shift (150 nm). The detection limit of this probe was as low as 7.1 nM based on $\text{S/N} = 3$. This probe exhibited a good performance in detecting Hg^{2+} in real water samples, living cells and organisms.

Introduction

Hydrogen mercury has been widely applied in various fields, such as electro-circuits, chemistry, medicine and biology. Mercury is very toxic to human beings and animals, and has been considered as one of the most dangerous pollutants in the environment.^{1,2} Mercury pollution is caused by natural events and human activities such as burning of coal.³ The use of mercury-containing pesticides and mercury-contaminated irrigation water can also lead to the absorption and enrichment of mercury in crops and agricultural products.⁴ Water-soluble mercury can be converted into methyl mercury (CH_3HgX , $\text{X} = \text{Cl}^-$, AcO^- , etc.) by bacteria, which can be absorbed by aquatic organisms such as fish.^{5–8} As a consequence, the main human exposure to mercury is by eating fish containing a high level of mercury. Also, mushrooms have the highest inorganic mercury concentration (up to 20 mg kg^{-1} of dry weight).⁹ The accumulation of mercury in the human body causes damage to the brain, nervous system, kidneys, endocrine and motion systems.^{5,10–12} Even the intake of a trace amount of mercury can also result in acute and chronic damage. As a result, the Environmental Protection Agency (EPA) has set the maximum level of Hg^{2+} in drinking water and food at 2 ppb (10 nM).^{6,12} Therefore, it is very important to develop rapid and effective methods for the detection of Hg^{2+} in the environment and biological systems. Conventional techniques have been successfully used to detect Hg^{2+} , including liquid

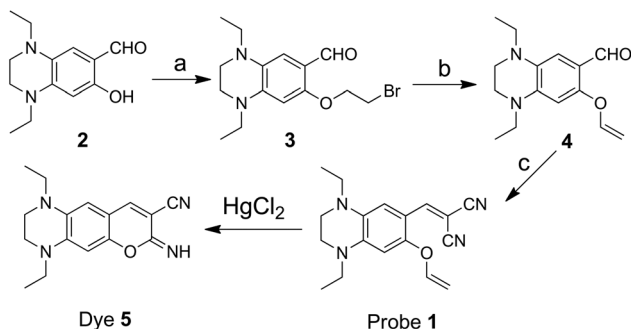
chromatography (HPLC),¹³ capillary electrophoresis (CE),¹⁴ atomic absorption spectroscopy (AAS), inductively coupled plasma mass spectroscopy (ICP-MS) and so on.^{15,16} While being useful, these methods are time-consuming, require expensive sophisticated instruments, or are subject to tedious sample preparation. In particular, none of these conventional methods can detect Hg^{2+} *in vivo*. In contrast, Hg^{2+} fluorescent probes have excellent selectivity and high sensitivity, operational simplicity and can be applied *in vivo*.¹⁷ In the past decade, a lot of fluorescent probes have been developed for the detection of Hg^{2+} .^{18–27} However, most of these probes have a high detection limit ($>30 \text{ nM}$), emission in a relatively short-wavelength spectral region and a small Stokes shift ($<100 \text{ nm}$) (Table S1†). In order to meet the standards of the EPA for determining Hg^{2+} , the detection limit of fluorescent probes should be under 10 nM. In addition, fluorescent dyes with emission in the red or near infrared (NIR) spectral region are more desirable for fluorescence detection because long-wavelength light can minimize the interference from the background, reduce photo-damage to biological samples and deeply penetrate tissues.^{28,29} What's more, fluorescent dyes with a large Stokes shift can avoid measurement error caused by self-absorption and scattering of excitation light.^{30,31}

Our previous study demonstrated that dye **5** is a good fluorophore to design fluorescent probes because of its long-wavelength emission ($\lambda_{\text{max}}^{\text{em}} = 625 \text{ nm}$), large Stokes shift (150 nm) and good water solubility. In this work, we used the precursor of dye **5** and a vinethene moiety as the sensing group to develop a fluorescent probe, **1**, for the selective detection of Hg^{2+} (Scheme 1). We anticipated that probe **1** would be non-fluorescent due to a strong photo-induced electron transfer (PET) process resulting from the vinethene moiety in the excited state; and the treatment of Hg^{2+} would selectively

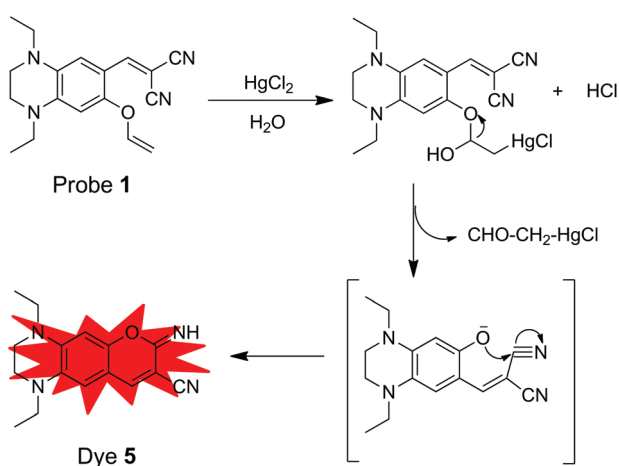
College of Chemistry & Chemical Engineering, Central South University, Changsha, Hunan Province, 410083, P. R. China. E-mail: song@rowland.harvard.edu

†Electronic supplementary information (ESI) available. See DOI: 10.1039/c8ob00831k

‡These authors contributed equally to this work.



Scheme 1 Synthesis of probe 1. (a) 1,2-Dibromoethane, K_2CO_3 , acetonitrile, reflux, 24 h. (b) Potassium *tert*-butoxide, DMSO, rt, 4 h. (c) Malononitrile, piperidine, EtOH, rt, 8 h.



Scheme 2 The sensing mechanism of probe 1 sensing for Hg^{2+} .

cleave the ether bond in probe 1 to release an intermediate, which would subsequently form fluorescent dye 5 through a cyclization reaction (Scheme 2).^{32–34}

Results and discussion

The sensitivity of probe 1 to Hg^{2+}

The sensing characteristic of probe 1 to Hg^{2+} was investigated in HEPES buffer (20 mM, pH = 7.4, containing 30% EtOH). The solution of probe 1 showed an absorption with a maximum at 495 nm and was hardly fluorescent as expected. Upon the addition of Hg^{2+} , the solution of probe 1 quickly produced a strong fluorescence with a maximum at 625 nm and the absorption spectrum blue-shifted to 475 nm. Remarkably, the fluorescence enhancement was up to 102-fold when excess Hg^{2+} was used. In the same media, dye 5 showed an emission with λ_{max}^{em} = 625 nm and an absorption centred at 475 nm. The optical behaviour of probe 1 with Hg^{2+} suggested that Hg^{2+} cleaved the vinethene moiety in probe 1 and resulted in the formation of dye 5 (Fig. 1, S1 and S2†).

In order to determine whether probe 1 can quantitatively detect Hg^{2+} , the solution of probe 1 (10.0 μ M) was treated with different concentrations of Hg^{2+} (0.0–60.0 μ M). As seen in Fig. 1 and 2, the fluorescence intensity at 625 nm proportionally increased with increasing the concentration of Hg^{2+} in a range of 0.0–20.0 μ M and the linearity was determined to be 0.996. The detection limit was 7.1 nM based on $S/N = 3$. When 5.0 equiv. of Hg^{2+} was used, the fluorescence signal reached a plateau. In addition, the quantitative detection of Hg^{2+} by probe 1 could be realized by monitoring its absorption spectral change, as shown in Fig. S3.†

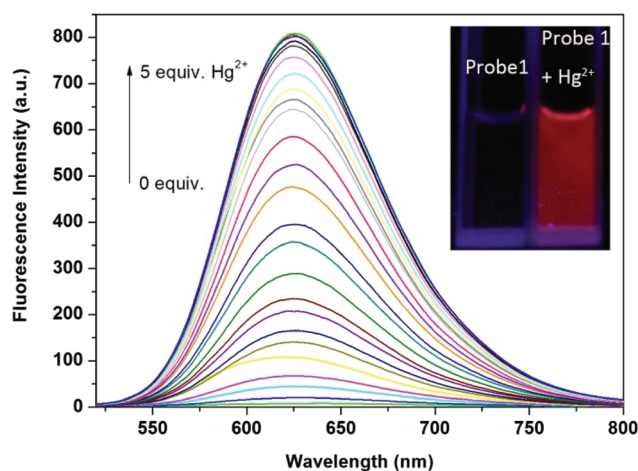


Fig. 1 Fluorescence spectra of probe 1 (10.0 μ M) upon the addition of Hg^{2+} (0.0–5.0 equiv.) in HEPES buffer (20 mM, pH = 7.4, containing 30% EtOH) at room temperature. Excitation wavelength: 475 nm. Excitation and emission slits: 5.0 nm/5.0 nm. Inset: Fluorescence photographs of probe 1 (left) and probe 1 with 5.0 equiv. of Hg^{2+} (right).

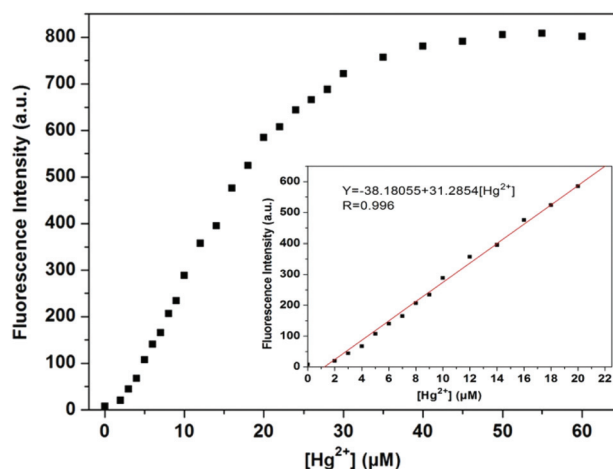


Fig. 2 Fluorescence intensity at 625 nm of probe 1 (10.0 μ M) versus Hg^{2+} concentration in HEPES buffer (20 mM, pH = 7.4, containing 30% EtOH). Inset: The linear relationship between the fluorescence intensity of probe 1 and Hg^{2+} concentration (0.0–20.0 μ M).

Sensing mechanism study

To further confirm the sensing mechanism (Scheme 2), HPLC analysis was performed on probe 1, dye 5 and the reaction solution of probe 1 with Hg^{2+} . probe 1 and dye 5 exhibited a single peak with retention times at 3.6 min (Fig. 3a) and 11.7 min (Fig. 3d), respectively. When 1.0 equiv. of Hg^{2+} was added into the solution of probe 1, the intensity of the peak at 3.6 min decreased with a concomitant occurrence of a new peak at 11.7 min (Fig. 3b). The addition of an excess of Hg^{2+} (5.0 equiv.) into the solution of probe 1 resulted in the disappearance of the peak at 3.6 min and only one peak at 11.7 min remained (Fig. 3c). Moreover, ^1H NMR and HRMS (Fig. S14–S15[†]) spectral analysis of the reaction product of probe 1 with Hg^{2+} clearly showed the formation of dye 5. The optical study, coupled with HPLC, NMR and HRMS analysis strongly supported the sensing mechanism proposed in Scheme 2.

Selectivity and competition studies

To explore the selectivity of probe 1, we investigated the fluorescence behaviour of probe 1 (10.0 μM) toward other cations (5.0 equiv.) in HEPES buffer (20 mM, pH = 7.4, containing 30% EtOH): NH_4^+ , Ba^{2+} , Ca^{2+} , Cd^{2+} , Cr^{3+} , Co^{2+} , Al^{3+} , K^+ , Mg^{2+} , Mn^{2+} , Na^+ , Ni^{2+} , Pb^{2+} , Fe^{3+} , Zn^{2+} , Cu^{2+} , Fe^{2+} , Sn^{2+} , and Pd^{2+} . As shown in Fig. 4, these interfering cations caused no fluorescence change. It is noteworthy that probe 1 still exhibited a good performance on detecting Hg^{2+} with the co-existence of these interfering cations (Fig. 5). These results strongly indicated that probe 1 could respond to Hg^{2+} with high selectivity.

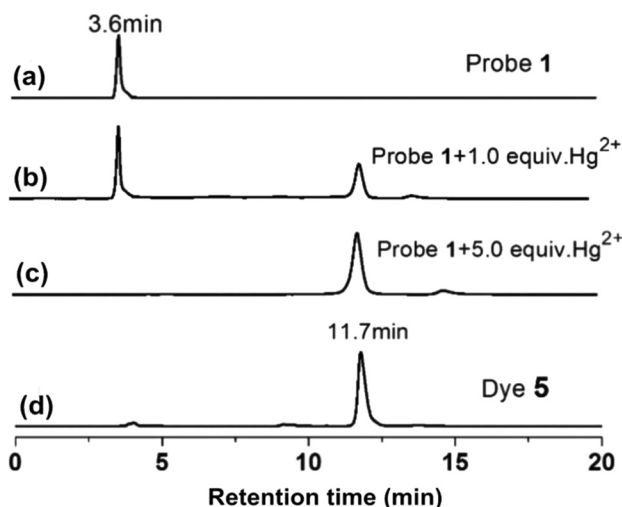


Fig. 3 HPLC chromatograms: probe 1 (50.0 μM) (a); probe 1 (50.0 μM) with 1.0 and 5.0 equiv. of Hg^{2+} incubated for 60 min in HEPES buffer (20 mM, pH = 7.4, containing 30% EtOH) (b) and (c); and dye 5 (50.0 μM) (d). Conditions: $\text{H}_2\text{O}/\text{CH}_3\text{CN}$ (v/v, 3/7); flow rate, 1.0 mL min^{-1} ; temperature, 25 $^{\circ}\text{C}$; detection wavelength, 475 nm; injection volume, 5.0 μL .

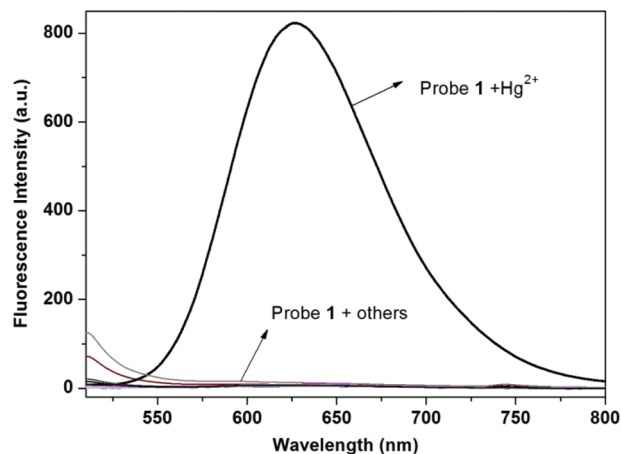


Fig. 4 Fluorescence spectra of probe 1 (10.0 μM) toward various other cations including NH_4^+ , Ba^{2+} , Ca^{2+} , Cd^{2+} , Cr^{3+} , Co^{2+} , Al^{3+} , K^+ , Mg^{2+} , Mn^{2+} , Na^+ , Ni^{2+} , Pb^{2+} , Fe^{3+} , Zn^{2+} , Cu^{2+} , Fe^{2+} , Sn^{2+} , and Pd^{2+} . Spectra were recorded after incubation for 60 min in HEPES buffer (20 mM, pH = 7.4, containing 30% EtOH).

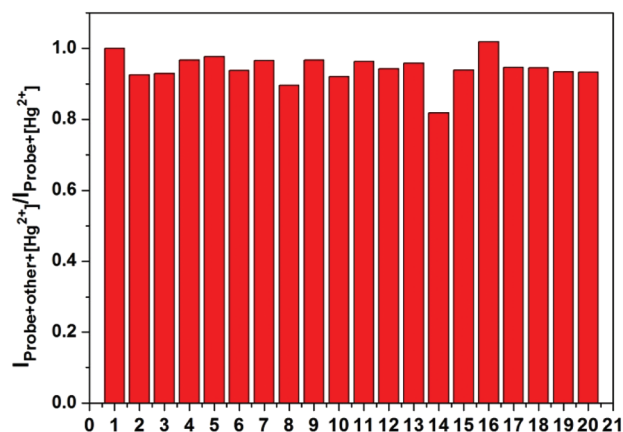


Fig. 5 Fluorescence intensity at 625 nm of probe 1 (10.0 μM) with Hg^{2+} (5.0 equiv.) with the co-existence of other cations (5.0 equiv.) in HEPES buffer (20 mM, pH = 7.4, containing 30% EtOH): (1) blank, (2) Cd^{2+} , (3) Cr^{3+} , (4) Co^{2+} , (5) K^+ , (6) Al^{3+} , (7) Na^+ , (8) Mg^{2+} , (9) Mn^{2+} , (10) Fe^{3+} , (11) Ni^{2+} , (12) Cu^{2+} , (13) Pb^{2+} , (14) Sn^{2+} , (15) NH_4^+ , (16) Zn^{2+} , (17) Fe^{2+} , (18) Ba^{2+} , (19) Ca^{2+} , and (20) Pd^{2+} .

Kinetic study

Time-dependent fluorescence experiments were conducted on probe 1 (10.0 μM) with Hg^{2+} (5.0 equiv.). Upon the addition of Hg^{2+} , the fluorescence intensity at 625 nm was enhanced along with the reaction time and a maximum was obtained within 60 min (Fig. 6). The result showed that the reaction between probe 1 and Hg^{2+} was first-order and the rate constant, k_{obs} , was 0.04579 min^{-1} (Fig. S13).[†]

pH effect studies

To determine whether probe 1 can function well in real samples, pH influence on the fluorescence behaviour of probe 1 toward Hg^{2+} (5.0 equiv.) was investigated (Fig. 7). The solu-

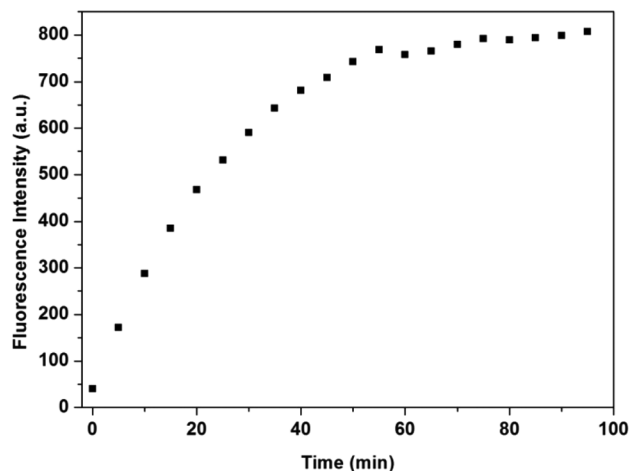


Fig. 6 Plot of fluorescence intensity at 625 nm of probe 1 (10.0 μM) with Hg^{2+} (5.0 equiv.) in HEPES buffer (20 mM, pH = 7.4, containing 30% EtOH) as a function of time.

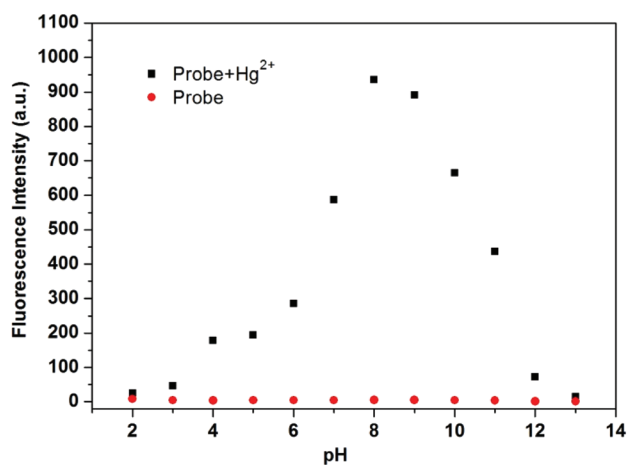


Fig. 7 pH effect on fluorescence intensity at 625 nm of probe 1 (10.0 μM) in the absence/presence of Hg^{2+} (5.0 equiv.) in HEPES buffer (20 mM, containing 30% EtOH).

tion of probe 1 showed a negligible fluorescence change in a pH range of 2–13. Upon the addition of Hg^{2+} (5.0 equiv.), the solution of probe 1 exhibited a strong red fluorescence between 6 and 11. These results suggested probe 1 had a potential application in detecting Hg^{2+} in environmental and biological samples.

Application of probe 1 to detect Hg^{2+} in water samples, living cells and organisms

In order to explore the application of probe 1 (10.0 μM), we utilized it to quantitatively determine Hg^{2+} in tap water, Yangtze River water and Xiang River water samples. All water samples were filtered through a 0.25 μM filter membrane, and then were spiked with different concentrations of Hg^{2+} (0.0, 2.0, 4.0, 6.0, 8.0, 10.0, 12.0, 14.0, 16.0, 18.0, and 20.0 μM). It's seen in Fig. 8a that there is a linear relationship between the fluo-

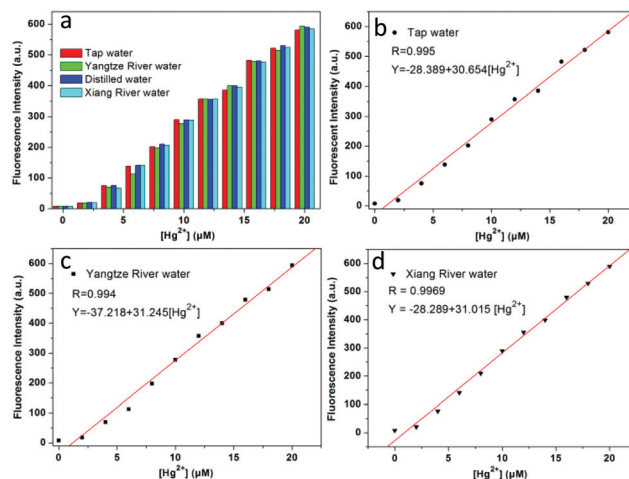


Fig. 8 (a) Fluorescence response of probe 1 (10.0 μM) in the presence of different concentrations of Hg^{2+} in water samples (20 mM HEPES buffer, pH = 7.4, 30% EtOH). (b), (c) and (d) Linear relationships of fluorescence intensity of probe 1 at 625 nm versus the spiked concentrations of Hg^{2+} (0.0–20.0 μM) in tap water, Yangtze River and Xiang River samples.

rescence intensity at 625 nm and Hg^{2+} concentration in real water samples (Fig. 8b–8d) with a recovery (Table S2).†

In addition, the potential application of probe 1 in detecting intracellular Hg^{2+} in living cells was evaluated. First, cytotoxic assays of probe 1 in HeLa cells were performed and 91% of cell viability was obtained when cells were treated with 10.0 μM of probe 1 for 24 h indicating probe 1 is non-toxic (Fig. S16).† When HeLa cells were incubated with probe 1 (10.0 μM) for 30 min and then treated with Hg^{2+} (50.0 μM) for another 30 min, an intense red fluorescence was displayed inside cells (Fig. 9). In contrast, when HeLa cells were incubated only with probe 1 (10.0 μM) for 30 min, negligible fluorescence was observed.

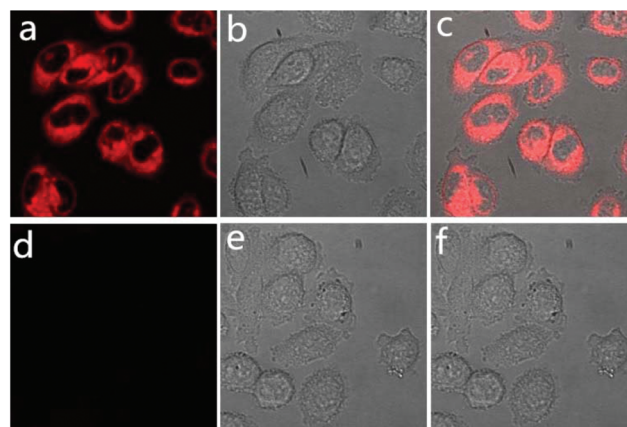


Fig. 9 Fluorescence (a, d), bright field (b, e) and merged (c, f) images of HeLa cells. Top row: Cells incubated with probe 1 (10.0 μM) and then treated with Hg^{2+} (50.0 μM). Bottom row: Cells incubated with probe 1 (10.0 μM).

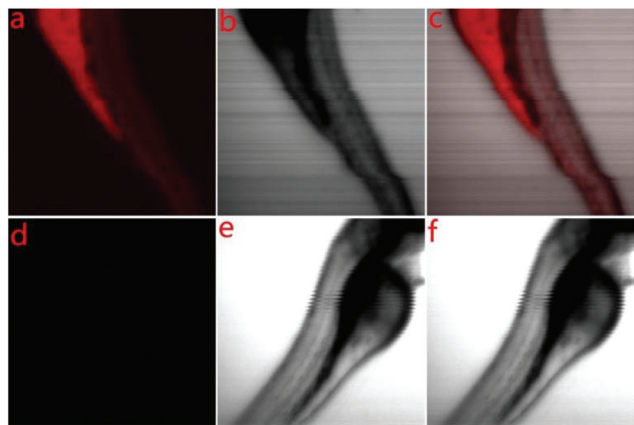


Fig. 10 Fluorescence (a, d), bright field (b, e) and merged (c, f) images of probe 1 in three-day old zebrafish. Top row: Zebrafish incubated with probe 1 (10.0 μM) and then treated with Hg^{2+} (50.0 μM). Bottom row: Zebrafish incubated with probe 1 (10.0 μM).

Finally, we used three-day old zebrafish to examine the ability of probe 1 to detect Hg^{2+} in living organisms. When zebrafish was incubated with probe 1 (10.0 μM) for 30 min at 28 $^{\circ}\text{C}$, and then treated with Hg^{2+} (50.0 μM) for another 30 min, a strong red fluorescence was observed (Fig. 10a). In contrast, the treatment of zebrafish with probe 1 did not induce any fluorescence (Fig. 10d).

Experimental section

Instruments and materials

All the reagents were purchased from commercial suppliers and were used without further purification. Mass spectra were obtained on a Bruker Daltonics micrOTOF-Q II mass spectrometer. ^1H NMR and ^{13}C NMR spectra were recorded on a Bruker 400 spectrometer and chemical shifts were reported as parts per million, using TMS as an internal standard. Fluorescence spectra were recorded on an F-280 fluorometer (Tianjin Gangdong Sci. & Tech. Development Co. Ltd). UV-Vis spectra were recorded on a UV-2450 spectrometer (Shimadzu). High performance liquid chromatography was carried out on a SPD-16 HPLC system (Shimadzu (Suzhou) Instruments Manufacturing, Co., Ltd). pH measurements were carried out on a Leici PHS-25 meter. A thin layer chromatography silica gel plate and silica gel (mesh 200–300) were supplied by Qingdao Ocean Chemicals, China. HeLa cells were provided by the State Key Laboratory of Chemo/Biosensing and Chemometrics, Hunan University. Zebrafish were provided by Nanjing Eze-Rinka Biotechnology Co., Ltd, China. All the experiments on living zebrafish were performed in compliance with the relevant local laws and institute guidelines, and the institution committee of Central South University has approved the experiments.

Synthesis of compound 2

Compound 2 was synthesized according to the literature method.³⁵

Synthesis of compound 3

Compound 2 (468 mg, 2 mmol) and 1,2-dibromoethane (1.5 g, 8 mmol) were dissolved in 30 mL acetonitrile, and then potassium carbonate (1.1 g, 8 mmol) was added to the solution. The mixture was refluxed for 20 hours under an argon atmosphere. Then the reaction mixture was cooled to room temperature. The solid was removed by filtration and was washed with 30 mL dichloromethane. The filtrate was distilled under vacuum and the obtained residue was purified by silica gel column chromatography using petroleum ether/ethyl acetate ($v/v = 4/1$) as an eluent to give compound 3 as a dark yellow solid (120 mg, 17.6% yield). HRMS (ESI) m/z : calcd for $\text{C}_{15}\text{H}_{21}\text{BrN}_2\text{O}_2\text{Na}$ $[\text{M} + \text{Na}]^+$, 363.0684; found, 363.0567. ^1H NMR (500 MHz, CDCl_3) δ 10.22 (s, 1H), 7.01 (s, 1H), 6.04 (s, 1H), 4.35 (t, $J = 6.2$ Hz, 2H), 3.67 (t, $J = 6.2$ Hz, 2H), 3.55–3.50 (m, 2H), 3.42 (q, $J = 7.1$ Hz, 2H), 3.34 (q, $J = 7.1$ Hz, 2H), 3.22–3.17 (m, 2H), 1.24 (t, $J = 7.1$ Hz, 3H), 1.18 (t, $J = 7.1$ Hz, 3H). ^{13}C NMR (125 MHz, CDCl_3) δ_c 186.8, 157.0, 143.2, 114.8, 108.6, 94.7, 69.9, 47.8, 45.7, 45.3, 44.8, 29.2, 10.8, 9.9.

Synthesis of compound 4

To a solution of compound 3 (120 mg, 0.38 mmol) in 5 mL DMSO was added potassium *tert*-butoxide (80 mg, 0.76 mmol). The mixture was stirred at room temperature under an argon atmosphere for 6 h. Next, the reaction mixture was poured into 150 mL distilled water and extracted with ethyl acetate (50 mL \times 3). The organic layers were combined and dried over anhydrous sodium sulphate. The organic solvent was evaporated under vacuum, and the residue was purified by silica gel column chromatography utilizing petroleum ether/ethyl acetate ($v/v = 4/1$) as an eluent to afford compound 4 as a yellow oil (60 mg, 60.7% yield). HRMS (ESI) m/z : calcd for $\text{C}_{15}\text{H}_{20}\text{N}_2\text{O}_2\text{Na}$ $[\text{M} + \text{Na}]^+$, 283.1422; found, 283.1281. ^1H NMR (400 MHz, CDCl_3) δ 10.08 (s, 1H), 7.01 (s, 1H), 6.66 (dd, $J = 13.8$, 6.1 Hz, 1H), 6.11 (s, 1H), 4.68 (dd, $J = 13.8$, 1.9 Hz, 1H), 4.41 (dd, $J = 6.1$, 1.9 Hz, 1H), 3.53 (dd, $J = 5.7$, 4.3 Hz, 2H), 3.44–3.38 (m, 2H), 3.38–3.33 (m, 2H), 3.23 (dd, $J = 5.7$, 4.3 Hz, 2H), 1.22 (t, $J = 5.8$ Hz, 3H), 1.19 (t, $J = 5.7$ Hz, 3H). ^{13}C NMR (100 MHz, CDCl_3) δ_c 186.7, 154.8, 150.0, 143.0, 131.0, 115.4, 107.6, 98.5, 94.1, 47.6, 45.7, 45.3, 44.7, 10.7, 9.9.

Synthesis of probe 1

To a solution of compound 4 (60 mg, 0.23 mmol) and malononitrile (30 mg, 0.45 mmol) in 10 mL EtOH was added 15 μL piperidine. The reaction mixture was stirred at room temperature for 8 h under an argon atmosphere. Then, the solvent was distilled under vacuum to give a residue, which was purified through silica gel column chromatography using dichloromethane/petroleum ether ($v/v = 2/1$) as an eluent to afford probe 1 as a red solid (45 mg, 63.6% yield). HRMS (ESI) m/z : calcd for $\text{C}_{18}\text{H}_{21}\text{N}_4\text{O}$ $[\text{M} + \text{H}]^+$, 308.1637; found, 308.1309. ^1H NMR (500 MHz, CDCl_3) δ 7.91 (s, 1H), 7.54 (s, 1H), 6.55 (dd, $J = 13.7$, 6.0 Hz, 1H), 6.09 (s, 1H), 4.79 (dd, $J = 13.7$, 2.0 Hz, 1H), 4.53 (dd, $J = 6.0$, 2.0 Hz, 1H), 3.64–3.54 (m, 2H), 3.45 (q, $J = 7.2$ Hz, 2H), 3.37 (q, $J = 7.1$ Hz, 2H), 3.30–3.24 (m, 2H),

1.28–1.21 (m, 6H). ^{13}C NMR (100 MHz, CDCl_3) δ_c 153.4, 150.1, 148.4, 144.3, 130.8, 117.2, 116.0, 110.7, 107.1, 97.3, 96.4, 68.8, 48.0, 46.1, 45.6, 44.5, 11.0, 9.8.

Synthesis of the reaction product of probe 1 with Hg^{2+}

HgCl_2 (62.3 mg, 0.25 mmol) was dissolved in 7 mL water, followed by the addition of the solution of probe 1 (15.5 mg, 0.05 mmol) in 3 mL EtOH. The mixture was stirred at room temperature for 2 h under an argon atmosphere. Then, the reaction mixture was extracted with dichloromethane (30 mL \times 3), and the organic layers were combined. After drying over anhydrous sodium sulphate, the organic solvent was removed under vacuum and the obtained residue was purified through silica gel column chromatography using ethyl acetate/dichloromethane (v/v = 1/1) as an eluent to give the desired product as a red solid (5.0 mg, 35.5% yield). ^1H NMR (500 MHz, CDCl_3) δ 7.59 (s, 1H), 6.36 (s, 1H), 6.32 (s, 1H), 3.60–3.54 (m, 2H), 3.45 (d, J = 7.2 Hz, 2H), 3.33 (d, J = 7.1 Hz, 2H), 3.29–3.23 (m, 2H), 1.28–1.19 (m, 6H).

Synthesis of dye 5

Dye 5 was synthesized according to the literature method.³⁶

Cell culture and fluorescence imaging experiments

HeLa cells were cultured in DEME medium supplemented with 10% fetal bovine serum and 1% penicillin at 37 °C for 24 h in an atmosphere containing 5% CO_2 . For cell imaging experiments, the nutrition medium was removed and cells were washed with PBS buffer three times. Next, the cells were treated with the solution of probe 1 (10.0 μM) for 30 min at 37 °C, washed three times with PBS buffer and further incubated with 50.0 μM Hg^{2+} for another 30 min. For a control experiment, cells were incubated only with probe 1 (10.0 μM) under the same conditions.

Zebrafish were provided by Nanjing Eze-Rinka Biotechnology Co., Ltd, China. All the experiments on living zebrafish were performed in compliance with the relevant local laws and institute guidelines, and the institution committee of Central South University has approved the experiments. Three-day old zebrafish were incubated with probe 1 (10.0 μM) in E3 embryo media (15 mM NaCl, 0.5 mM KCl, 1 mM MgSO_4 , 1 mM CaCl_2 , 0.15 mM KH_2PO_4 , 0.05 mM Na_2HPO_4 , 0.7 mM NaHCO_3 , 10^{−5}% methylene blue; pH 7.5) for 30 min at 28 °C. Zebrafish were washed with E3 media and were further incubated with 50.0 μM Hg^{2+} in E3 media for 30 min at 28 °C. For the control experiment, zebrafish were only incubated with probe 1 (10.0 μM) under the same conditions. Before imaging experiments, zebrafish were washed with E3 media.

Conclusions

In summary, we have designed and synthesized a fluorescent probe for selective and sensitive detection of Hg^{2+} with a red emission, a low detection limit (7.1 nM) and a large Stokes

shift (150 nm). The preliminary application of this probe in detecting Hg^{2+} was demonstrated *in vitro* and *in vivo* for environmental and biological samples.

Conflicts of interest

There are no conflicts to declare.

Acknowledgements

This work was supported by the National Natural Science Foundation of China (no. U1608222), the State Key Laboratory of Fine Chemicals (KF1606) and the State Key Laboratory of Chemo/Biosensing and Chemometrics (2016005).

Notes and references

- 1 P. Grandjean, P. Weihe, R. F. White and F. Debes, *Environ. Res.*, 1998, **77**, 165–172.
- 2 T. C. Hutchinson, K. M. Meema and W. O. M. Cycling, *Lead, mercury, cadmium and arsenic in the environment*, Published on behalf of the Scientific Committee on Problems of the Environment (Scope) of the Intern, 1987.
- 3 C. Jadán-Piedra, M. Baquedano, S. Puig, D. Vélez and V. Devesa, *J. Agric. Food Chem.*, 2017, **65**, 2876–2882.
- 4 S. E. Lindberg, D. R. Jackson, J. W. Huckabee, S. A. Janzen, M. J. Levin and J. R. Lund, *J. Environ. Qual.*, 1979, **8**, 572–578.
- 5 M. Harada, *Crit. Rev. Toxicol.*, 1995, **25**, 1–24.
- 6 H. H. Harris, I. J. Pickering and G. N. George, *Science*, 2003, **301**, 1203.
- 7 S. Jonsson, U. Skyllberg, M. B. Nilsson, P. O. Westlund, A. Shchukarev, E. Lundberg and E. Björn, *Environ. Sci. Technol.*, 2012, **46**, 11653–11659.
- 8 F. Wang, R. W. Macdonald, D. A. Armstrong and G. A. Stern, *Environ. Sci. Technol.*, 2012, **46**, 11821–11828.
- 9 P. Kalač and L. r. Svoboda, *Food Chem.*, 2000, **69**, 273–281.
- 10 F. Baldi, M. Filippelli and G. J. Olson, *Microb. Ecol.*, 1989, **17**, 263–274.
- 11 J. Gutknecht, *J. Membr. Biol.*, 1981, **61**, 61–66.
- 12 E. M. Nolan and S. J. Lippard, *Chem. Rev.*, 2008, **108**, 3443–3480.
- 13 L. Liu, Y.-W. Lam and W.-Y. Wong, *J. Organomet. Chem.*, 2006, **691**, 1092–1100.
- 14 J. Chen, H. Chen, X. Jin and H. Chen, *Talanta*, 2009, **77**, 1381–1387.
- 15 Y. Li, C. Chen, B. Li, J. Sun, J. Wang, Y. Gao, Y. Zhao and Z. Chai, *J. Anal. At. Spectrom.*, 2005, **21**, 94–96.
- 16 M. Puanngam, P. K. Dasgupta and F. Unob, *Talanta*, 2012, **99**, 1040–1045.
- 17 G. Singh, S. I. Reja, V. Bhalla, D. Kaur, P. Kaur, S. Arora and M. Kumar, *Sens. Actuators, B.*, 2017, **249**, 311–320.
- 18 M. G. Choi, Y. H. Kim, J. E. Namgoong and S.-K. Chang, *Chem. Commun.*, 2009, **0**, 3560–3562.

- 19 M. Dong, Y.-W. Wang and Y. Peng, *Org. Lett.*, 2010, **12**, 5310–5313.
- 20 Y. Feng, Z. Kuai, Y. Song, J. Guo, Q. Yang, Y. Shan and Y. Li, *Talanta*, 2017, **170**, 103–110.
- 21 M. Hong, S. Lu, F. Lv and D. Xu, *Dyes. Pigm.*, 2016, **127**, 94–99.
- 22 M. Kumar, S. I. Reja and V. Bhalla, *Org. Lett.*, 2012, **14**, 6084–6087.
- 23 D. Li, C.-Y. Li, Y.-F. Li, Z. Li and F. Xu, *Anal. Chim. Acta*, 2016, **934**, 218–225.
- 24 W. Lin, X. Cao, Y. Ding, L. Yuan and L. Long, *Chem. Commun.*, 2010, **46**, 3529–3531.
- 25 M. Santra, B. Roy and K. H. Ahn, *Org. Lett.*, 2011, **13**, 3422–3425.
- 26 G. Zhang, D. Zhang, S. Yin, X. Yang, Z. Shuai and D. Zhu, *Chem. Commun.*, 2005, **0**, 2161–2163.
- 27 B. Zhu, W. Wang, L. Liu, H. Jiang, B. Du and Q. Wei, *Sens. Actuators, B*, 2014, **191**, 605–611.
- 28 Z. Guo, S. Park, J. Yoon and I. Shin, *Chem. Soc. Rev.*, 2014, **43**, 16–29.
- 29 L. Yuan, W. Lin, K. Zheng, L. He and W. Huang, *Cheminform*, 2013, **42**, 622–661.
- 30 X. Peng, F. Song, E. Lu, Y. Wang, W. Zhou, A. Jiangli Fan and Y. Gao, *J. Am. Chem. Soc.*, 2005, **127**, 4170–4171.
- 31 L. Yuan, W. Lin and H. Chen, *Biomaterials*, 2013, **34**, 9566–9571.
- 32 Y. S. Cho and K. H. Ahn, *Tetrahedron Lett.*, 2010, **51**, 3852–3854.
- 33 Q. Fang, Q. Liu, X. Song and J. Kang, *Luminescence*, 2016, **30**, 1280–1284.
- 34 A. Wang, Y. Yang, F. Yu, L. Xue, B. Hu, W. Fan and Y. Dong, *Talanta*, 2015, **132**, 864–870.
- 35 W. Chen, Q. Fang, D. Yang, H. Zhang, X. Song and J. Foley, *Anal. Chem.*, 2014, **87**, 609–616.
- 36 L. Yang, Y. Su, Z. Sha, Y. Geng, F. Qi and X. Song, *Org. Biomol. Chem.*, 2018, **16**, 1150–1156.